Exceeding probability analysis for rail of high-speed railway under seismic excitations

Hongping Xing
School of civil engineering, Southwest Jiaotong University, Chengdu, China
Yu Liu
School of civil engineering, Southwest Jiaotong University, Chengdu, China and Key Laboratory of High-speed Railway Engineering of Ministry of Education, Southwest Jiaotong University, Chengdu, China, and
Xiaodan Sun
School of civil engineering, Southwest Jiaotong University, Chengdu, China and National Engineering Research Center for Geological Disaster Prevention Technology in Land Transportation, Southwest Jiaotong University, Chengdu, China

Received 11 August 2023
Revised 15 September 2023
Accepted 18 September 2023

Abstract

Purpose – The smoothness of the high-speed railway (HSR) on the bridge may exceed the allowable standard when an earthquake causes vibrations for HSR bridges, which may threaten the safety of running trains. Indeed, few studies have evaluated the exceeding probability of rail displacement exceeding the allowable standard. The purposes of this article are to provide a method for investigating the exceeding probability of the rail displacement of HSRs under seismic excitation and to calculate the exceeding probability.

Design/methodology/approach – In order to investigate the exceeding probability of the rail displacement under different seismic excitations, the workflow of analyzing the smoothness of the rail based on incremental dynamic analysis (IDA) is proposed, and the intensity measure and limit state for the exceeding probability analysis of HSRs are defined. Then a finite element model (FEM) of an assumed HSR track-bridge system is constructed, which comprises a five-span simply-supported girder bridge supporting a finite length CRTS II ballastless track. Under different seismic excitations, the seismic displacement response of the rail is calculated; the character of the rail displacement is analyzed; and the exceeding probability of the rail vertical displacement exceeding the allowable standard (2mm) is investigated.

Findings – The results show that: (1) The bridge-abutment joint position may form a step-like under seismic excitation, threatening the running safety of high-speed trains under seismic excitations, and the rail displacements at mid-span positions are bigger than that at other positions on the bridge. (2) The exceeding probability of rail displacement is up to about 44% when PGA = 0.01g, which is the level-five risk probability and can be described as 'very likely to happen'. (3) The exceeding probability of the rail at the mid-span positions is bigger than that above other positions of the bridge, and the mid-span positions of the track-bridge system above the bridge may be the most hazardous area for the running safety of trains under seismic excitation when high-speed trains run on bridges.

This work is supported by National Key Research and Development Plan of China "Basic Theory and Methods for Resilience Assessment and Risk Control of Transportation Infrastructures" (2021YFB2600500), the National Nature Science Foundation of Si Chuan (2023NSFSC0388) and the Joint Research Fund for Earthquake Science launched by the National Natural Science Foundation of China and China Earthquake Administration (U2039208).

Railway Sciences
Vol. 2 No. 4, 2023
pp. 413-430
Emerald Publishing Limited
e-ISSN: 2755-0915
p-ISSN: 2755-0907
DOI 10.1108/RS-08-2023-0027

Originality/value – The work extends the seismic hazardous analysis of HSRs and would lead to a better understanding of the exceeding probability for the rail of HSRs under seismic excitations and better references for the alert of the HSR operation.

Keywords Workflow, Incremental dynamic analysis, Dynamic displacement response, The smoothness of the rail, Exceeding probability, Risk level

Paper type Research paper

1. Introduction

The mileage of the high-speed railway (HSR) is rapidly extending, and they have become the focal point of future development (Sheng, Zheng, Zhu, Luo, & Zheng, 2020; Song, Liu, Cui, Yu, & Li, 2020). HSRs mainly operate on bridges (Wang, 2011) to mitigate the effect of various climatic, geological and other conditions. Due to their extensive coverage and high-density operations, many HSR lines inevitably traverse high-intensity areas. The rail irregularity under seismic excitation can deteriorate safety, passenger comfort (Zhai, 2020) and interaction with other infrastructures (Song, 2021). Consequently, rail displacement under seismic excitation exceeding the allowable standard poses a severe threat to the safety of high-speed trains.

The rail of the China HSRs maintains rigorous smoothness requirements for vertical displacement, a critical factor in the smoothness of the rail. Ensuring that the vertical displacement of the rail remains within the allowable standard is essential for ensuring the safety of high-speed trains during seismic excitation. The prescribed standard for rail vertical displacement on China HSRs, operating at design speeds of 200–350 km/h, is ±2 mm (TG/GW 115-2012, 2012). Numerous studies have been conducted to address the rail dynamic displacement regularities on the bridge, considering the influence of the bridge system (Wang, 2011; Zhu, Yang, Wang, Cai, & Dai, 2017; He, 2019), track system (Wu, 2018; Yan, Li, Liu, & Xie, 2021; Yu *et al.*, 2021; Lv, 2021) and seismic characters (Yu *et al.*, 2021; Lv, 2021; Xue, 2018; Jin, Pei, Li, Liu, & Qiang, 2016; Li, Hong, Lei, & Liu, 2015; Wang, 2014; Lei, 2014). Moreover, earthquake cannot be reproduced because it is a single random process with considerable variability and uncertainty (Li, Yu, Mao, & Spencer, 2021). Conventional dynamic analysis may not establish a direct connection between ground motion intensity and the level of structural damage, making it challenging to estimate the dynamic capacity of the rail against earthquake load accurately. In this context, vulnerability analysis emerges as a suitable method, employing vulnerability curves to address the probability of structures exceeding the allowable standard. This approach enables a more comprehensive evaluation of rail resilience to seismic forces.

Indeed, there is a scarcity of studies evaluating the exceeding probability of the earthquake-induced displacement of the rail exceeding the allowable standard, in contrast to the extensive research on the vulnerability analysis of other components in the HSR track-bridge system (Jin *et al.*, 2016; Cheng *et al.*, 2020; Wei *et al.*, 2022; Liang, Yan, Zhao, Wang, & Zang, 2022), along with other structures (Xiao, 2013; Zhang, 2014; Liang, Zhu, Zhu, Du, & Wang, 2021; Lv, Su, & Zhou, 2012; Ding, Zi, Ji, Shi, & Ren, 2020). For instance, the vulnerability of the bridge (Cheng *et al.*, 2020; Wei *et al.*, 2022; Liang *et al.*, 2022), ballastless track structure (Wei *et al.*, 2022) and wheels uplift from the rail (Jin *et al.*, 2016) have been extensively investigated. At present, the incremental dynamic analysis (IDA) introduced by Bertero (1977) is extensively employed to assess the vulnerability of structures. The IDA offers several advantages, as it allows for a step-by-step and incremental scaling of ground motion records (Bertero, 1977). Moreover, it provides a more accurate estimation of the dynamic capacity of structures against seismic loads (Dadkhah, Kamgar, & Heidarzadeh, 2022; Dadkhah, Kamgar, Heidarzadeh, Jakubczyk-Gałczyńska, & Jankowski, 2020). Seismic vulnerability curves can be calculated using the IDA, depicting the correlation between the

ground motion intensity and the extent of structural damage. These curves serve as a powerful tool for evaluating structural seismic risk.

In this paper, the workflow of analyzing the smoothness of the rail based on IDA is proposed for calculating the exceeding probability of the rail displacement exceeding the allowable standard under various seismic excitations. The intensity measure and limit state are also defined for evaluating the exceeding probability in the context of HSRs. Subsequently, a finite element model (FEM) of an assumed HSR track-bridge system is constructed in ABAQUS, which comprises a five-span simply-supported girder bridge supporting a finite length CRTS II ballastless track. Through the use of this FEM, the seismic displacement response of the rail is calculated under different seismic excitations. The character of the rail displacement is thoroughly analyzed to gain insights into its behaviour during seismic events. The exceeding probability of the rail vertical displacement exceeding the allowable standard is investigated.

2. Methodology

The workflow of analyzing the smoothness of the rail based on IDA (Wei *et al.*, 2022; Hwang and Liu, 2004; GB 50111-2006, 2006; GB50011-2010, 2010) is proposed for calculating the exceeding probability of the rail displacement exceeding the allowable standard under various earthquake excitations, as illustrated in Figure 1. Conventional IDA (Wei *et al.*, 2022; Cui *et al.*, 2021) involves gradually scaling the intensity of ground motion records to multiple levels until the structure reaches a state of destruction, which is evaluated using predefined damage rules. The endpoint of IDA, where structures are destroyed, is unsuitable for assessing the exceeding probability of the rail. In order to investigate this probability, the

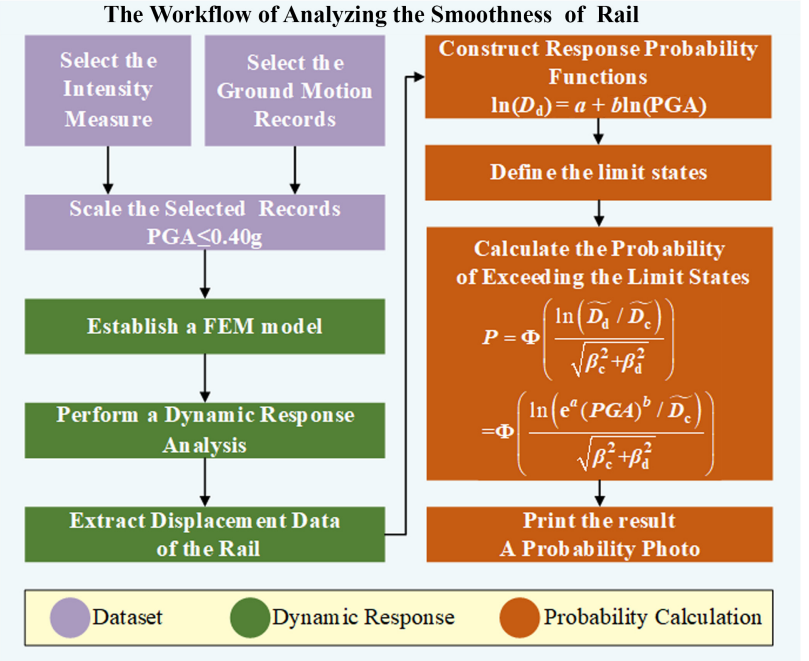

Source(s): Author's own work

Figure 1.
The workflow of analyzing the smoothness of the rail

dataset employs peak ground acceleration (PGA) as the intensity measure of the ground motion records, following the guidelines outlined in the Code for Seismic Design of Railway Engineering (GB 50111-2006, 2006). The PGA of ground motion records is scaled within the range of PGA≤0.40g, following the Code for Seismic Design of Buildings (GB50011-2010, 2010). This scaling allows for obtaining extensive rail displacement data under earthquakes of varying intensity levels. For probability calculation, linear regression is employed to model the relationship between the logarithm of PGA and the logarithm of the vertical displacement of the rail (Hwang & Liu, 2004). The exceeding probability can be defined using a standard normal cumulative distribution function (Wei *et al.*, 2022; Hwang & Liu, 2004). The rail displacement amplitude is then fed into these mathematical models to calculate the exceeding probability of the rail.

Where D_d is the rail vertical displacement of (mm); a and b are the fitted equation coefficients; $\widetilde{D_d}$ is the structure average response, which can be calculated by the regression analysis; $\widetilde{D}_c$ is the average structural total bearing capacity, which can be determined by the limit state of the rail vertical displacement; e is the natural constant; β_d is the logarithmic standard deviation of structural reaction; β_c is the logarithmic standard deviation of structural bearing capacity; $\Phi(x)$ is the standard normal cumulative distribution function.

3. Dataset

3.1 Select ground motion records

The ground motion record plays a crucial role as input in the IDA. In the first attempt to evaluate the exceeding probability of the rail dynamic displacement under seismic excitation, great earthquakes are selected according to the standard magnitude in the China Earthquake Network. All chosen ground motion records are near-fault motions, ensuring high seismic intensity. Moreover, earthquakes are selected according to Chandler's classification (Kamgar & Rahgozar, 2020) across all three categories in order to have a chance to create more critical responses to the railway system on the bridge. All the criteria (GB50011-2010, 2010; Kamgar & Rahgozar, 2020) for selecting ground motion records are provided in Table 1. Subsequently, the ground motion records are chosen from five different earthquakes in the PEER NGA-West2 strong ground motion dataset, as indicated in Table 2. Due to space constraints, Figure 2 displays only three records. Additionally, all ground motion records are represented by labels, as presented in Table 2. For instance, one of the horizontal components of the Chalfant Valley 02 at the Bishop LADWP South St station is denoted as 'LAD180', a simplified representation derived from the file name of the record obtained from the PEER. Each ground motion record consists of two horizontal components, such as 'LAD180' and 'LAD270', and one vertical component, such as 'LAD-UP.' Figure 3 illustrates the response

Criteria	Ranges
M_w	≥6
R_{JB}	<25 km
PGA (GB50011-2010, 2010)	>0.05 g
PGA/PGV (Kamgar & Rahgozar, 2020)	<0.8 (g s/m)
	0.8 (g s/m) ≤ PGA/PGV≤1.2 (g s/m)
	PGA/PGV>1.2 (g s/m)

Table 1.
Criteria for selecting ground motion records

Source(s): Authors' own work

Earthquakes	Stations	Labels	M_W	R_{JB} (km)	PGA (g)	PGV (m/s)	PGA/PGV (g s/m)
Chalfant Valley 02	Bishop LADWP South St	LAD180	6.19	14.38	0.25	0.20	1.25
		LAD270			0.18	0.20	0.90
		LAD-UP			0.14	0.07	2.00
Kobe Japan	Kakogawa	KAK000	6.90	22.5	0.24	0.21	1.14
		KAK090			0.32	0.27	1.19
		KAK-UP			0.17	0.11	1.55
Coalinga 01	Pleasant Valley P.P. yard	PVY045	6.36	7.69	0.60	0.60	1.00
		PVY135			0.53	0.39	1.36
		PVY-UP			0.37	0.16	2.31
Superstition hills 02	Westmorland Fire Sta	WSM090	6.54	13.03	0.17	0.23	0.74
		WSM180			0.21	0.32	0.66
		WSM-UP			0.23	0.09	2.56
Imperial valley 02	El Centro Array #9	ELC180	6.95	6.09	0.28	0.31	0.90
		ELC270			0.21	0.31	0.68
		ELC-UP			0.18	0.09	2.00

Source(s): Authors' own work

Table 2.
Ground motion records selected from PEER

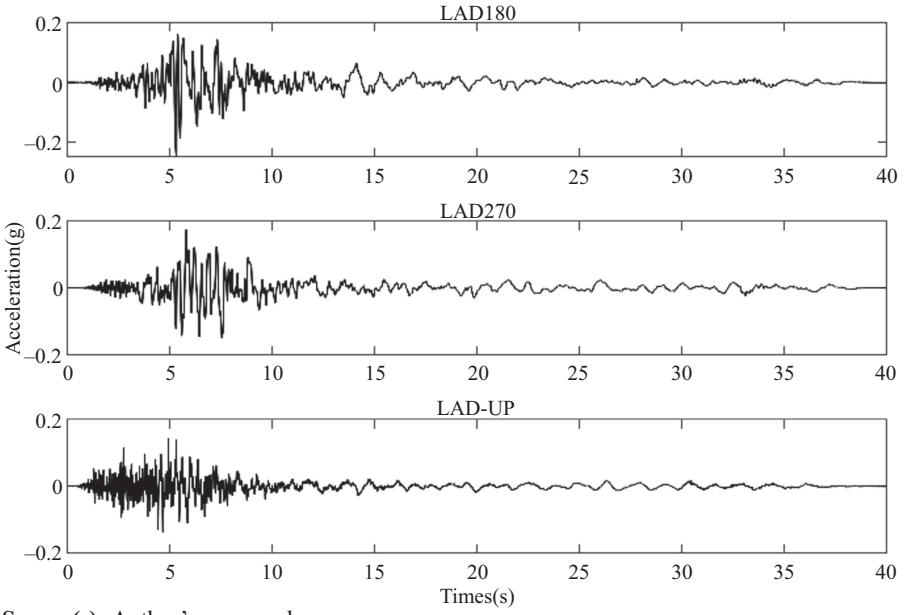

Source(s): Author's own work

Figure 2.
The records of 'LAD180'/'LAD270'/'LAD-UP'

spectra of these selected ground motions, depicting their spectral content and highlighting their differences.

3.2 Scale the selected records

In this research paper, a group consisting of one horizontal and one vertical component is inputted in the FEM, represented by the horizontal component. To illustrate, the group

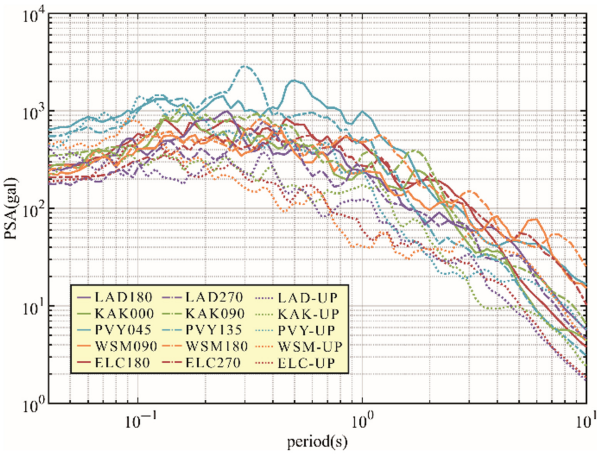

Figure 3.
Response spectra of these selected ground motions

Source(s): Author's own work

'LAD180' + 'LAD-UP' is represented by 'LAD180'. Consequently, all ground motion records are categorized into ten distinct groups. The horizontal component of an earthquake is applied in the x direction, which aligns with the orientation of the bridge, while the vertical component is simultaneously applied in the y direction, perpendicular to the bridge, as depicted in Figure 4. In order to study exceeding probability, the PGA of ground motion records in each group is scaled to the following levels of PGA = 0.01g, 0.025g, 0.05g, 0.10g, 0.15g, 0.20g, 0.25g, 0.30g, 0.35g and 0.40g, respectively. Consequently, 100 seismic excitations are generated and inputted into the bottom of the piers for analysis.

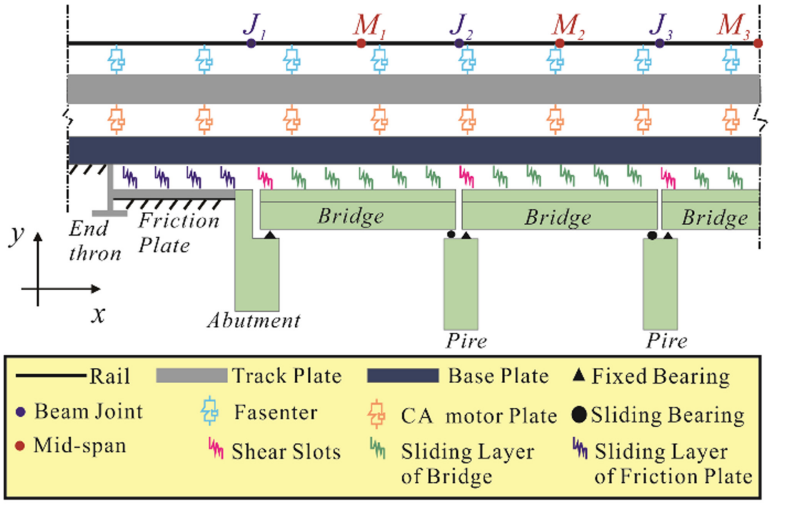

Figure 4.
FEM and selected positions of the high-speed railway track-bridge system

Source(s): Author's own work

4. Dynamic response of high-speed railway track-bridge system under seismic excitation

4.1 FEM of high-speed railway track-bridge system

A high proportion of the HSRs in China rely on the CRTS II slab ballastless track structure (CRTS II SBTS) (Li, 2016), which is a crucial system element, particularly on bridges. In order to model this scenario, a 2-D FEM of a HSR track-bridge system incorporating the CRTS II SBTS is developed using ABAQUS. Specifically, the model includes a 5-span simply supported girder bridge, oriented in the direction x, as depicted in Figure 4. The bridge deck comprises five single box sections, each measuring 32.4 m long, constructed from C50-grade concrete. The pier is 8 m high and made of C35-grade concrete. The rail is 282.1 m long, made of 60 kg/m steel and connected to the track structure through fasteners spaced at intervals of 0.65 m. The CRTS II SBTS comprises three layers from bottom to top: the base plate, the CA mortar layer and the track slab. The track slab is a 0.2-m-thick precast slab made of C60-grade concrete, while the base plate is a 0.19-m-thick slab made of C40-grade concrete. A 0.03-m-thick CA mortar layer is filled between the track slab and the base plate. The rail, track slab, base plate and pier are represented by beam elements in the FEM. The fastener between the rail and the track slab, the CA mortar layer between the track and base plate, the sliding layer of friction plate between the base plate and friction plate, as well as the shear slots and the sliding layer of bridge between the track slab and the base plate, are simulated by spring elements. The stiffness, damping and yield displacement values of those springs for various components are provided in Table 3 (Jiang *et al.*, 2020; Gwo, Li, & Liu, 2018; Lei, 2015; Chen, Jiang, Yu, & Zeng, 2012). For the seismic response comparison, six positions are selected on the rail-track-bridge system, including three joints between beams (J_1, J_2 and J_3) and three mid-span positions (M_1, M_2 and M_3), as illustrated in Figure 4.

4.2 Vertical displacement of the rail

The vertical displacements of the rail at six selected positions are compared under 100 seismic excitations. Nevertheless, due to space constraints, Figure 5 illustrates the vertical displacements of the rail at four selected positions under three seismic excitations. In Figure 5, the red and thin lines denote the vertical displacement of the rail at position J_1, while the green and thick lines denote the vertical displacements of the rail at positions J_2, M_1 and M_3.

As depicted in Figure 5, the rail displacements at positions M_1, J_2 and M_3 are larger than the displacement observed at position J_1. This phenomenon is particularly notable when the rail displacement is negative, while it is unnotable when it is positive. Additionally, the rail displacements at positions M_1, J_2 and M_3 are relatively comparable. This behaviour can be attributed to the longitudinal continuity of the CRTS II SBTS. The proximity of position J_1 to the subgrade leads to its displacement being constrained by the CRTS II SBTS above the subgrade. Figure 5 suggested that under seismic excitation, the rail at position J_1, which is also the girder-subgrade joint, may exhibit a step-like displacement pattern. This phenomenon indicates a potential deterioration in the smoothness of the high-speed rail, posing a threat to the running safe of high-speed trains.

4.3 The vertical displacement amplitude of the rail

According to Figure 1, the vertical displacement amplitude of the rail plays a crucial role in analyzing its behaviour. In order to illustrate this, Figure 6 displays the vertical displacement amplitude of the rail under seismic excitation of various intensity levels. Due to space constraints, only the vertical displacement amplitudes of thirty cases are presented in Figure 6. Furthermore, Figure 7 illustrates the average values of the vertical displacement amplitudes of the rail at six selected positions.

Direction	Component	Stiffness		
		F-D relationship (kN/mm)	F (kN)	D (mm)
Longitudinal	Fastener	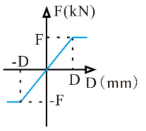	15	2.00
	CA mortar		42	0.50
	Sliding layer of bridge		6	0.50
	Shear slots		1465	0.12
	Fixed bearing		1000	2.00
	Sliding bearing		100	2.00
	Sliding layer of friction plate		14	2.00
	Foundation	72	/	/
Direction	**Component**	**Stiffness(kN/mm)/ F-D relationship/value**		**Damping (kN·s/m)**
Vertical	Fastener	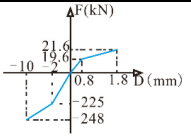		47.7
	CA mortar	1080		100
	Sliding layer of bridge	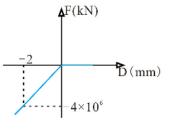		/
	Shear slots	Rigid		/
	Fixed bearing	Rigid		3.475×10^3
	Sliding bearing	Rigid		3.475×10^3
	Sliding layer of friction plate	1080		/
	Foundation	72		108

Source(s): Author's own work

Table 3.
Stiffness, damping, yield force and yield displacement of the adopted springs

The vertical displacement amplitudes of the rail vary under different seismic excitations, even when their PGA are the same. This difference in displacement amplitude increases with PGA. Remarkably, even at a relatively low PGA of 0.01g, the vertical displacement amplitude of the rail can also exceed the threshold of 2 mm specified in the TG/GW 115-2012 Maintenance Rules for Ballastless Track of High-Speed Railway (TG/GW 115-2012, 2012). Furthermore, a general regularity is observed: the vertical displacement amplitude of the rail at the mid-point of the span is greater than that at the beam joint. Figures 6 and 7 demonstrate that the rail displacement amplitude differs for each seismic excitation, potentially leading to the vertical displacement amplitude of the rail exceeding the limit state (TG/GW 115-2012, 2012), even though the PGA = 0.01*g*. This phenomenon indicates that the mid-span position may be possibly the more vulnerable and hazardous position for the rail under seismic excitations when high-speed trains run on bridges.

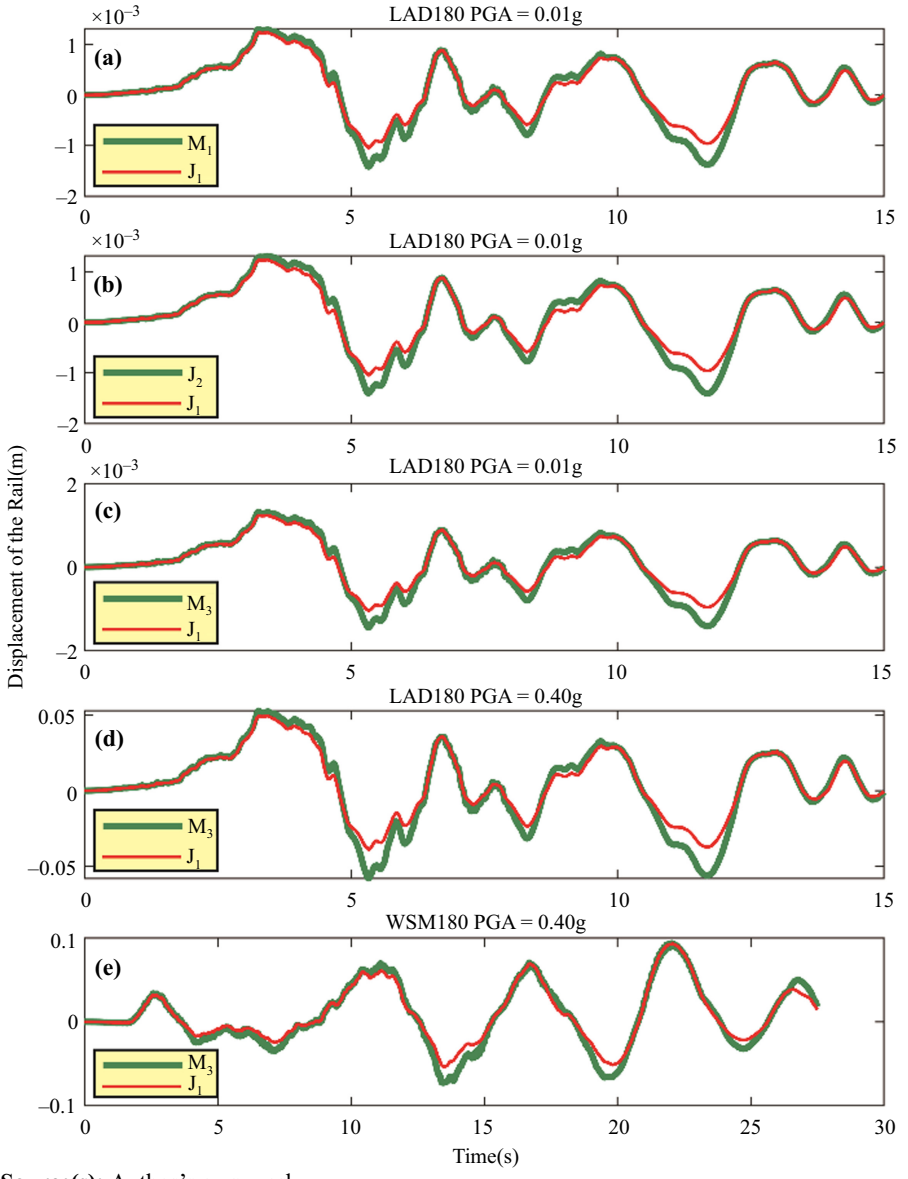

Source(s): Author's own work

Figure 5.
The vertical displacement of the rail at four selected positions under three cases

5. The probability of the rail displacement exceeds the limit value

5.1 Construct response probability function of the rail displacement under seismic excitation

In this research paper, the general linear regression equation (Hwang & Liu, 2004) between the logarithm of PGA and the logarithm of the rail vertical displacement amplitude is provided in Figure 1 and Formula (1). The linear regression results are further presented in

Figure 6.
The vertical displacement amplitude of the rail

Source(s): Author's own work

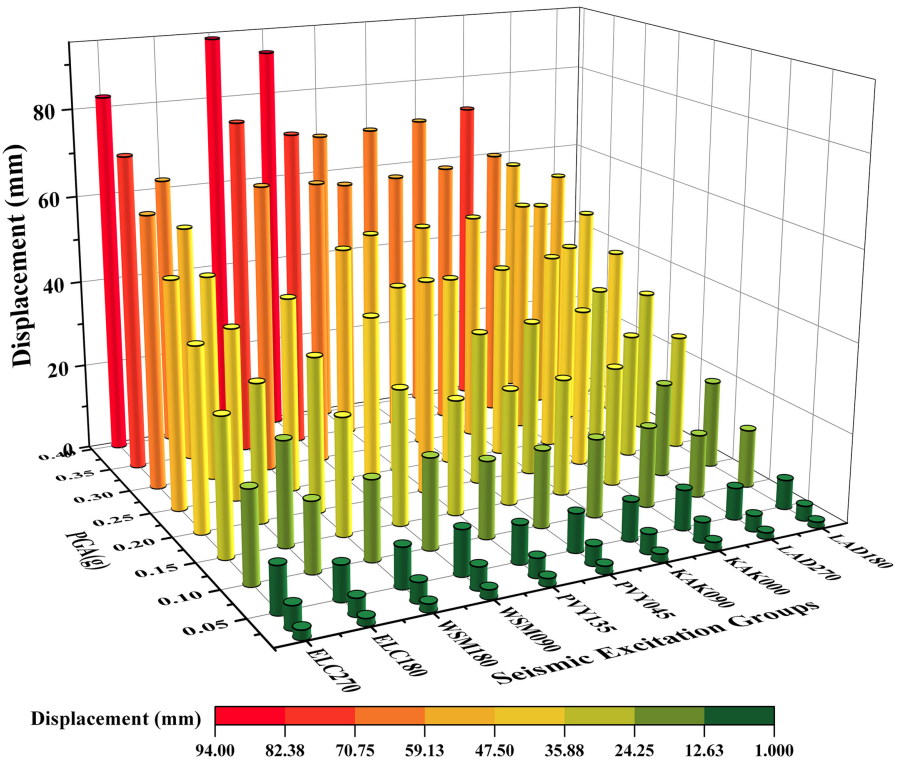

Source(s): Author's own work

Figure 7.
The average values of the vertical displacement amplitude of the rail at six positions

Figure 8. In Figure 8, the solid color lines denote the fitting curves of the rail displacement at six selected positions, while the black points correspond to the logarithmic values of the vertical displacement amplitude of the rail. Figure 8 reveals that linear regression equation coefficients for the rail displacement at selected six positions are similar. The R-square, which serves as a deviation coefficient indicating the correlation degree in the linear regression function, is found to be above 0.98. That indicates an excellent fit of the regression results, suggesting a strong correlation between the logarithm of PGA and the logarithm of the vertical displacement amplitude of the rail at each position.

$$\ln(D_{\mathrm{d}}) = A + B\ln(\mathrm{PGA}) \tag{1}$$

Where D_{d} is the rail vertical displacement (mm); A and B are the fitted equation coefficients.

5.2 The exceeding probability of the rail displacement under seismic excitation

High-speed railways have strict requirements for smoothness and as such, a vertical displacement of the rail not exceeding 2 mm is selected as the limit state (TG/GW 115-2012, 2012), represented as $\widetilde{D}_{\mathrm{c}} = 2\mathrm{mm}$. Then, the exceeding probability of rail displacement under seismic excitation can be calculated using the standard normal cumulative distribution function (Wei *et al.*, 2022; Hwang & Liu, 2004). The equation is provided in Figure 1 and Formula (2).

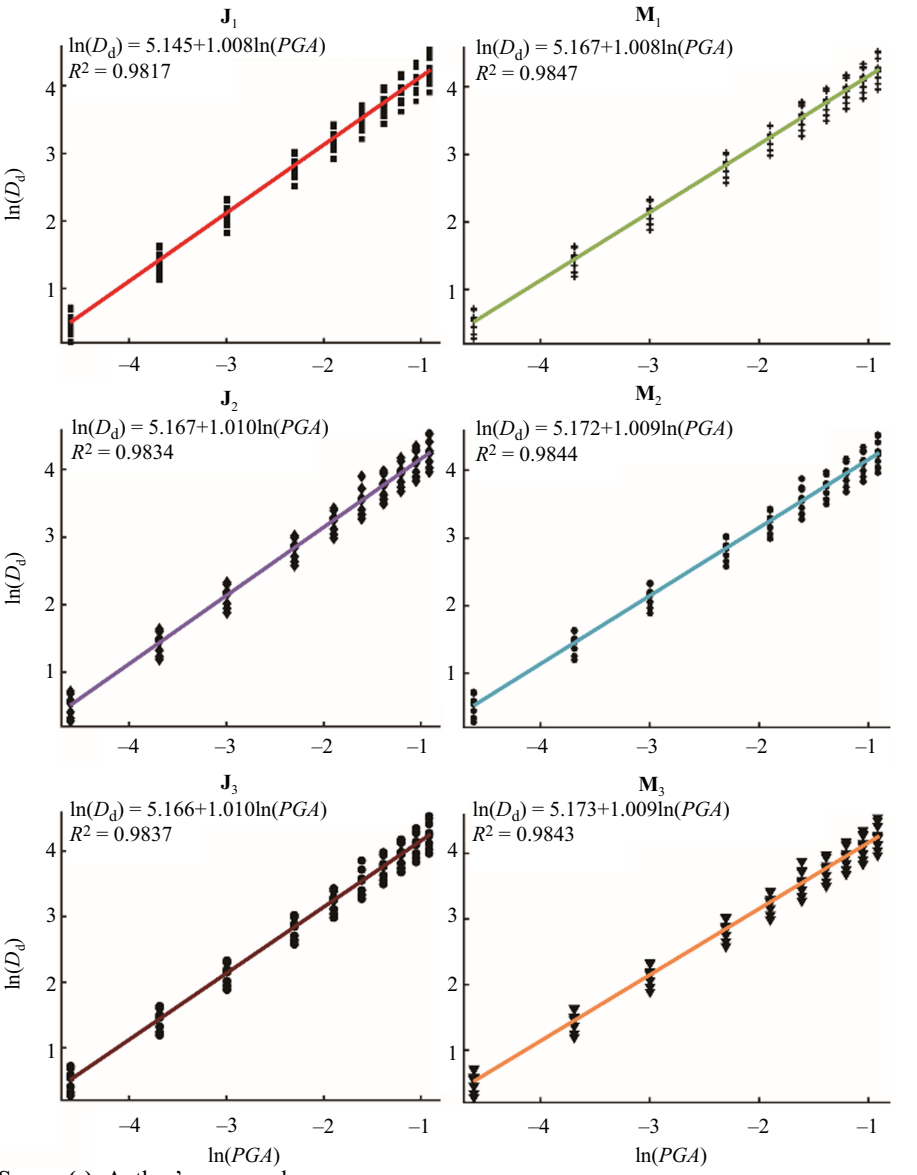

Figure 8.
The linear regression equations of the rail displacement at six positions

Source(s): Author's own work

$$P = \Phi\left(\frac{\ln\left(\widetilde{D}_{\mathrm{d}}/\widetilde{D}_{\mathrm{c}}\right)}{\sqrt{\beta_{\mathrm{c}}^2+\beta_{\mathrm{d}}^2}}\right) = \Phi\left(\frac{\ln\left(\mathrm{e}^{A}(PGA)^{B}/\widetilde{D}_{\mathrm{c}}\right)}{\sqrt{\beta_{\mathrm{c}}^2+\beta_{\mathrm{d}}^2}}\right) \tag{2}$$

Where $\widetilde{D_d}$ is the structure average response, which can be calculated by the regression analysis; $\widetilde{D_c}$ is the average of structural total bearing capacity, which can be defined by the limit state of the rail vertical displacement; e is the natural constant; β_d is the logarithmic standard deviation of structural reaction; β_c is the logarithmic standard deviation of structural bearing capacity; $\Phi(x)$ is the standard normal cumulative distribution function.

Figure 9 displays the exceeding probability curves of the rail displacement under seismic excitation at six selected positions. The legends in the figure represent the values of certain input parameters of the standard normal cumulative distribution function shown in Figure 1, and the solid color lines depict the exceeding probability curves of the rail vertical displacement exceeding 2mm.

As depicted in Figure 9, several important observations can be made: (1) The exceeding probabilities of the rail displacement exceeding 2 mm under seismic excitation at J_1 to M_3 are 43.66%, 44.38%, 44.09%, 44.40%, 44.05% and 44.43%, respectively, when the PGA is 0.01g. Moreover, the exceeding probability of rail displacement increases with PGA. (2) The exceeding probability of the rail displacement at J1 is the lowest, while the exceeding probability of the rail displacement at the mid-span points of the bridge (positions M_1, M_2 and M_3) is bigger than that at the beam joints of the bridge (positions J_1, J_2 and J_3). (3) The exceeding probabilities of the rail displacement increase from 0 to about 89% when the PGA increases from 0.00 to 0.05g. Overall, Figure 9 illustrates that the smoothness of the rail may deteriorate rapidly when a HSR track-bridge system is subjected to seismic excitation. Additionally, the mid-span points may be possibly the more vulnerable and hazardous positions for the rail, emphasizing the importance of considering these factors in the design and maintenance of HSR systems to ensure their safety and stability.

Besides, according to Table 4, the exceeding probability of rail displacement exceeding 30% can be described as 'very likely to happen' (Tie Jian She [2007], 2008; Q/CR 9006-2014, 2015). Additionally, Figure 9 demonstrates that the rail displacement is very likely to exceed 2 mm even when the PGA is as low as 0.01g. These findings underscore the potential significant threat earthquakes pose to the safety of high-speed train operations.

Figure 10 presents the exceeding probabilities of the rail displacement exceeding 2 mm under seismic excitations at six selected positions. The labels PGA = 0.05g, 0.10g, 0.20g and 0.40g on the Y-axis, marked with a yellow box at the bottom, correspond to the PGA of four seismic fortification intensities. The correspondences between seismic fortification intensities and basic design seismic acceleration are shown in Table 5 (GB50011-2010, 2010; GB 500111-2006, 2006).

Figure 10 provides further evidence that the exceeding probability of the rail displacement exceeding 2 mm at the mid-span points of the bridge (positions M_1, M_2 and M_3) is consistently bigger than that at the beam joints of the bridge (positions J_1, J_2 and J_3) under seismic excitation with PGA = 0.01g to 0.40g. Although the exceeding probabilities of the rail displacement exceeding 2 mm differ at various positions, the maximum difference between them is approximately 2%. Notably, under seismic excitation with PGA = 0.05g, which corresponds to the basic design seismic acceleration associated with China's lowest seismic fortification intensity, the exceeding probabilities of the rail displacement exceeding 2 mm at all six selected positions are above 88%. This probability is significantly well above the fifth-risk probability level and can be described as 'very likely to happen.'

6. Conclusion

In this paper, the workflow of analyzing the smoothness of the rail based on IDA is proposed for calculating the exceeding probability of the rail displacement exceeding the allowable standard under various earthquake excitations and elaborated according to the practical

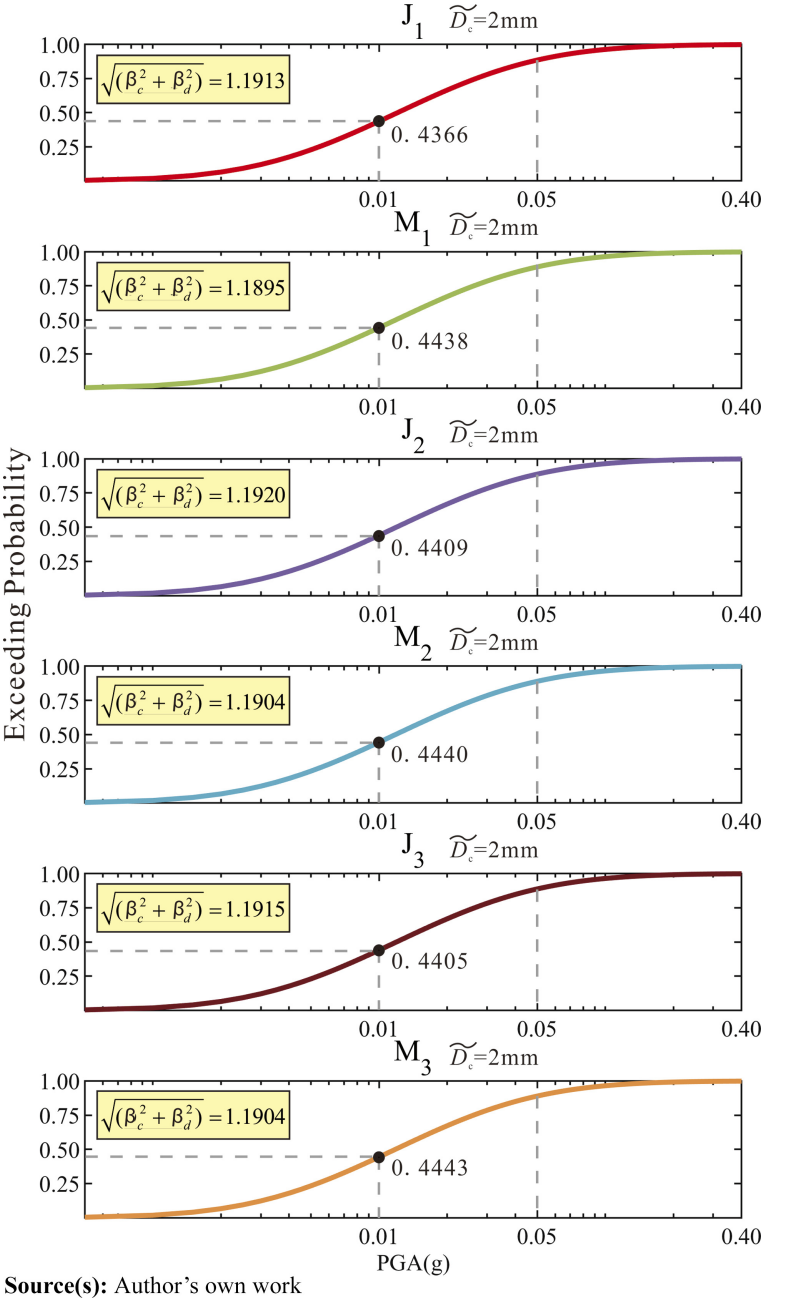

Source(s): Author's own work

Figure 9.
The exceeding probability curves of the rail displacement under seismic excitation at six positions

example, which extends the seismic hazardous analysis of HSRs. Then the seismic displacement response of the rail is calculated, the character of the rail displacement is

analyzed, and the exceeding probability of the rail vertical displacement exceeding the allowable standard (2mm) is investigated under different seismic excitations. The main conclusions include:

Ranges	Descriptions	Levels
>0.3	Very likely	5th
0.03~0.3	Likely	4th
0.003~0.03	Roughly even chances	3th
0.0003~0.003	Unlikely	2th
≤0.0003	Very unlikely	1th

Note(s): '~' means that the ranges include the upper limit value but not the lower limit value
Source (s): Authors' own work

Table 4.
The risk probability classification

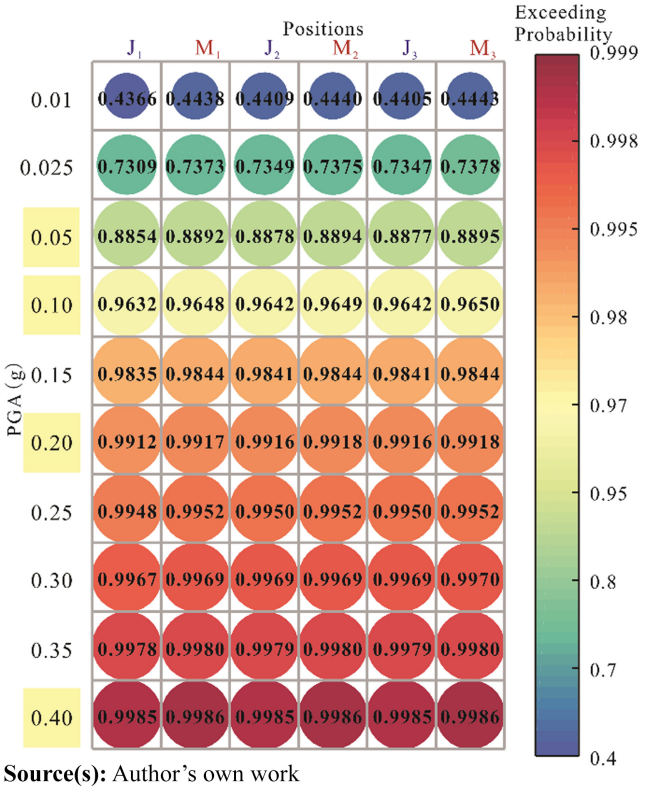

Source(s): Author's own work

Figure 10.
The exceeding probability of the rail displacement exceeding 2 mm under seismic excitation at six positions

Seismic fortification intensities	*6*	*7*	*8*	*9*
Basic design seismic acceleration (g)	0.05	0.10	0.20	0.40

Source(s): Authors' own work

Table 5.
The correspondences between seismic fortification intensities and basic design Seismic acceleration

(1) For the exceeding probability analysis of HSRs, the workflow of analyzing the smoothness of the rail is proposed, and the intensity measure and limit state are also defined.

(2) The bridge-abutment joint position may form a step-like hazardous area that threatens the safety of high-speed trains running under seismic excitation. Moreover, the rail displacement at mid-span points is bigger than that at other bridge positions.

(3) Even though the PGA = 0.01g, the rail displacement may exceed 2 mm and the exceeding probability of the rail displacement is up to about 44%, which is the level-five risk probability, so the rail displacement exceeding 2 mm can be considered very likely to open.

(4) The exceeding probabilities of the rail displacement at mid-span points are bigger than those at other positions on the bridge. Therefore, the mid-span positions of the track-bridge system above the bridge may be the more hazardous area for the safety of trains running under seismic excitation when high-speed trains run on bridges.

References

Bertero, V. V. (1977). Strength and deformation capacities of buildings under extreme environments. *Structural Engineering and Structural Mechanics*, *53*(1), 29–79.

Chen, L., Jiang, L., Yu, Z., & Zeng, Z. (2012). Numerical analysis of the seismic responses of round-ended piers of high-speed railway bridges. *Journal of Hunan University*, *39*(4), 18–24.

Cheng, W., Wang, G., Du, Y., Cao, Y., Xu, R., & Guo, J. (2020). Vulnerability analysis of the continuous high-speed railway bridge under near-fault earthquake. *Journal of Harbin Engineering University*, *41*, 212–218.

Cui, M., Wang, C., Chen, C., Pan, Y., Xiongh, Y., & Ren, C. (2021). Seismic fragility analysis on existing high-rise shear-wall structure based on incremental dynamic analysis. *Building Science*, *37*, 151–157.

Dadkhah, M., Kamgar, R., Heidarzadeh, H., Jakubczyk-Gałczyńska, A., & Jankowski, R. (2020). Improvement of performance level of steel moment-resisting frames using tuned mass damper system. *Applied Sciences*, *10*(10), 3403.

Dadkhah, M., Kamgar, R., & Heidarzadeh, H. (2022). Reducing the cost of calculations for incremental dynamic analysis of building structures using the discrete wavelet transform. *Journal of Earthquake Engineering*, *26*(7), 3317–3342.

Ding, Z., Zi, H., Ji, X., Shi, C., & Ren, Z. (2020). Seismic fragility analysis of mountain tunnels considering lining degradation. *Chinese Journal of Rock Mechanics and Engineering*, *39*(3), 581–592.

GB 50111-2006 (2006). *GB 50111-2006 Code for seismic design of railway engineering*. Beijing, China: Planning Press.

GB50011-2010 (2010). *GB50011-2010 Code for seismic design of Buildings*. Beijing, China: Architecture and Building Publishing.

Gwo, W., Li, J., & Liu, H. (2018). The analysis of running safty of high-speed-train on bridge by using refined simulation considering strong earthquake. *Engineering Mechnaics*, *35*(S1), 259–264+277.

He, B. (2019). *Study on dynamic response of CRTS II ballastless track structure on bridge under earthquake*. Beijing, China: Beijing Jiaotong University.

Hwang, H., & Liu, J. (2004). Seismic fragility analysis of reinforced concrete bridges. *China Civil Engineering Journal*, *37*(06), 47–51.

Jiang, L., Yu, J., Zhou, W., Yan, W., Lai, Z., & Feng, Y. (2020). Applicability analysis of high-speed railway system under the action of near-fault ground motion. *Soil Dynamics and Earthquake Engineering*, *139*, 106289.

Jin, Z., Pei, S., Li, X., Liu, H., & Qiang, S. (2016). Effect of vertical ground motion on earthquake-induced derailment of railway vehicles over simply-supported bridges. *Journal of Sound and Vibration*, *383*, 277–294.

Kamgar, R., & Rahgozar, P. (2020). Optimum location for the belt truss system for minimum roof displacement of teel buildings subjected to critical excitation. *Steel and Composite Structures*, *37*(4), 463–479.

Lei, H. (2014). *Coupling vibration and running safety of train-track-bridge system under non-uniform seismic excitation*. Chengdu, China: Southwest Jiaotong University.

Lei, X. (2015). *High speed railway track dynamics: Model, algorithm and application*. Beijing, China: Science Press.

Li, D. (2016). *Performance of CRTS II slab ballastless track on the high speed railway bridge*. Beijing, China: China Academy of Railway Science.

Li, X., Hong, Q., Lei, H., & Liu, Z. (2015). Effect of input directions of seismic ground motion on seismic responses of a railway extradosed bridge. *Bridge Construction*, *45*(1), 26–32.

Li, H., Yu, Z., Mao, J., & Spencer, B. F. (2021).Effect of seismic isolation on random seismic response of High-Speed railway bridge based on probability density evolution method. *Structures*, *29*, 1032–1046.

Liang, Y., Zhu, J., Zhu, R., Du, J., & Wang, Y. (2021). Seismic fragility analysis of RCC-RC composite bridge with high-strength steel bar. Word Earthquake. *Engineering*, *37*(03), 85–93.

Liang, Y., Yan, S., Zhao, B., Wang, Y., & Zang, C. (2022). Seismic vulnerability analysis of near-fault high-speed railway rigid-frame bridge. *Journal of Zhengzhou University (Engineering Science)*, *43*(04), 80–85+91.

Lv, J. (2021). *Research on dynamic performance of bridge-track system with simple supported beams on high-speed railway under pulsed near fault ground motion*. Chongqing, China: Chongqing Jiaotong University.

Lv, X., Su, N., & Zhou, Y. (2012). IDA-based seismic fragility analysis of a complex high-rise structure. *Earthquake Engineering and Engineering Vibration*, *32*(05), 19–25.

Q/CR 9006-2014 (2015). *Q/CR 9006-2014 technical Code for risk management of railway construction engineering*. Beijing, China: China Railway Publishing House.

Sheng, X., Zheng, W., Zhu, Z., Luo, T., & Zheng, Y. (2020). Properties of rubber under-ballast mat used as ballastless track isolation layer in high-speed railway. *Construction and Building Materials*, *240*, 117822.

Song, L., Liu, H., Cui, C., Yu, Z., & Li, Z. (2020). Thermal deformation and interfacial separation of a CRTS II slab ballastless track multilayer structure used in high-speed railways based on meteorological data. *Construction and Building Materials*, *237*, 117528.

Song, Y., Wang, Z., Liu, Z., & Wang, R. (2021). A spatial coupling model to study dynamic performance of pantograph-catenary with vehicle-track excitation. *Mechanical Systems and Signal Processing*, *151*, 107336.

TG/GW 115-2012 (2012). *TG/GW 115-2012 maintenance Rules for ballastless track of high speed railway*. Beijing, China: China Railway Publishing House.

Tie Jian She [2007] (2008). *Temporary regulations of railway tunnel risk assessment and management*. Beijing, China: China Railway Publishing House.

Wang, G. (2011). *The mechanics characteristics of ballastless track on bridge during earthquake*. Beijing, China: Beijing Jiaotong University.

Wang, W. (2014). *Research on seismic response of track-bridge system considering wave passage effect*. Beijing, China: China Academy of Railway Science.

Wei, B., Wang, W., Wang, P., Yang, T., Jiang, L., & Wang, T. (2022). Seismic responses of a high-speed railway (HSR) bridge and track simulation under longitudinal earthquakes. *Journal of Earthquake Engineering*, *26*(9), 4449–4470.

Wu, S. (2018). *Response and optimization of CRTS II ballastless track structure under earthquake*. Beijing, China: Beijing Jiaotong University.

Xiao, M. (2013). *Seismic vulnerability analysis for concrete continuous rigid bridge with high piers*. Chengdu, China: Southwest Jiaotong University.

Xue, D. (2018). *Seismic performance analysis of high-speed railway bridges under near-fault earthquake*. Beijing, China: Beijing Jiaotong University.

Yan, B., Li, Z., Liu, S., & Xie, H. (2021). Seismic response of CRTS II ballastless track-bridge system considering the damage of track structure. *Science Progress*, *104*(3), 00368504211035207.

Yu, M., Lv, J., Jia, H., Jia, K., Zheng, S., & Zhao, C. (2021). Response analysis of high-speed railway bridge-rail system subjected to near-fault pulse-type earthquake. *Journal of Hunan Univiversity*, *48*(9), 138–146.

Zhai, W. (2020). *Vehicle–track coupled dynamics models* (pp. 17–149). Singapore: Springer Singapore.

Zhang, S. (2014). *Seismic vulnerability analysis for bridge structures with high piers*. Chengdu, China: Southwest Jiaotong University.

Zhu, Z., Yang, L., Wang, L. D., Cai, C. B., & Dai, G. (2017). Dynamic responses and train running safety of railway cable-stayed bridge under earthquakes. *Engineering Mechanics*, *34*(4), 78–87.

Corresponding author
Yu Liu can be contacted at: liuyu@swjtu.edu.cn